OAK RIDGE NATIONAL LABORATORY

MANAGED BY UT-BATTELLE, LLC.
POST OFFICE BOX 2008, OAK RIDGE, TENNESSEE 37831-6079

ORNL
CENTRAL FILES NUMBER

ORNL/CF-00/12

DATE: April 26, 2000

SUBJECT: Quarterly Technical Progress Report of Radioisotope Power System Materials Production and Technology Program Tasks for January through March 2000

TO: Distribution

FROM: J. P. Moore J.P. Moore

The enclosed revised report covers the second quarter of FY 2000. This report is one of a series to inform the Office of Space and Defense Power Systems, U.S. Department of Energy, and their contractors of accomplishments of the tasks covered by UT-Battelle. If you have any questions or require further clarification on any topic, please contact us at Building 4508, Mail Stop 6079.

JPM:dlm

UCN-2383
(3 6-88)

QUARTERLY TECHNICAL PROGRESS REPORT OF RADIOISOTOPE POWER SYSTEM MATERIALS PRODUCTION AND TECHNOLOGY PROGRAM TASKS FOR JANUARY THROUGH MARCH 2000

Prepared for Department of Energy
Office of Space and Defense Power Systems
under Budget and Reporting Classification
AF 70 10 20 0, AF 70 60 00 0, and AF 70 30 00 0

by

Radioisotope Power System Program
Metals and Ceramics Division
Oak Ridge National Laboratory

Oak Ridge National Laboratory
Oak Ridge, Tennessee 37831-6080
operated by UT-Battelle, LLC
for the
U.S. Department of Energy
Contract DE-AC05-00OR22725

This page intentionally blank

CONTENTS

This page intentionally left blank

QUARTERLY TECHNICAL PROGRESS REPORT OF RADIOISOTOPE POWER SYSTEM MATERIALS PRODUCTION AND TECHNOLOGY PROGRAM TASKS* FOR JANUARY THROUGH MARCH 2000

1. INTRODUCTION

The Office of Space and Defense Power Systems (OSDPS) of the Department of Energy (DOE) provides Radioisotope Power Systems (RPS) for applications where conventional power systems are not feasible. For example, radioisotope thermoelectric generators were supplied by the DOE to the National Aeronautics and Space Administration for deep space missions including the Cassini Mission launched in October of 1997 to study the planet Saturn. The Oak Ridge National Laboratory (ORNL) has been involved in developing materials and technology and producing components for the DOE for more than three decades. For the Cassini Mission, for example, ORNL was involved in the production of carbon-bonded carbon fiber (CBCF) insulator sets, iridium alloy blanks and foil, and clad vent sets (CVSs) and weld shields (WSs).

This quarterly report has been divided into three sections to reflect program guidance from OSDPS for fiscal year (FY) 2000. The first section deals primarily with maintenance of the capability to produce flight quality carbon-bonded carbon fiber (CBCF) insulator sets, iridium alloy blanks and foil, clad vent sets (CVSs), and weld shields (WSs). In all three cases, production maintenance is assured by the manufacture of limited quantities of flight quality (FQ) components. The second section deals with several technology activities to improve the manufacturing processes, characterize materials, or to develop technologies for two new RPS. The last section is dedicated to studies of the potential for the production of 238Pu at ORNL.

2. PRODUCTION TASKS

2.1 CARBON-BONDED CARBON FIBER

The goal of this effort is to maintain production capability for CBCF insulation sets. These are produced under closely controlled conditions and stringent QA procedures to ensure compliance with material specifications at each step in the production process, from the handling of raw materials to shipment of finished parts. Dedicated facilities for CBCF production remain in the Carbon and Insulation Materials Technology Laboratory. Periodic exercise of production activities is performed to assure that the processes can be successfully executed and to verify personnel competencies, and adequacy of training, equipment, and procedures.

Our goals this year include (1) complete the fabrication and characterization of CBCF sleeves initiated in FY 1999; (2) produce and certify nine new sets of flight-quality CBCF sleeves and disks; (3) initiate the qualification of a new, commercially available resin by producing nine sets of sleeves and disks to the current flight-quality specification; (4) consolidate the storage of CBCF raw materials, archive specimens, and completed sets into a room designated the CBCF Laboratory to allow for greater control and exclusive use of facilities; and (5) prepare a comprehensive video of all CBCF production and qualification tasks.

2.1.1 CBCF Production Activities

The graphite tube furnace used for CBCF carbonization and heat treatments is 12 years old and had been experiencing some electrical problems. It was determined that the nonconductive anodized layer inside the aluminum furnace shell had degraded and the electronics had drifted out of acceptable limits. The furnace was reanodized and all hoses, gaskets, and electrical insulators replaced. The SCR was replaced and the furnace controller tuned. The furnace was brought back into full operation in February.

Seven CBCF sleeves were machined from billets produced in FY 1999. Five met the flight-quality dimensional requirements. A new back-up machinist initiated training on these sleeves. A new inspector in our Metrology Department was qualified to perform dimensional inspection of CBCF sleeves and disks.

Two vacuum-molding runs of CBCF sleeves, each consisting of nine billets, and one plate run for CBCF disks were completed using available fibers and the qualified phenolic resin (Durez 22352). From these molding runs we will attempt to produce 18 flight-quality sleeves and 36 flight-quality disks. Two additional molding runs of CBCF sleeves will be made using the new commercial resin (Oxychem Durez 5034). Eighteen CBCF sleeves will be made using these billets. The balance of production and qualification activities (i.e., heat treatment, machining, metrology, x-ray, chemistry, etc.) will be carried out concurrently or consecutively to minimize set-up time and average cost of each component.

2.1.2 Inventory of Critical Materials

An inventory was conducted on the materials required for CBCF production. Raw materials on hand include:

1. Chopped and carbonized rayon fiber: 4.4 lbs., sufficient for 5 molding runs;
2. Chopped rayon fiber: 662 lbs., sufficient for 15 molding runs after carbonization;
3. Unchopped rayon tow: 2030 lbs., sufficient for 450 molding runs after chopping and carbonization;
4. Phenolic resin (Durez 22352): 20 lbs., sufficient for 30 molding runs.

2.1.3 Videotaping of CBCF Production and Qualification Tasks

Production of CBCF components is both an art and a science. Much of the science is specified in very detailed procedures that are followed for each step in the production and qualification of CBCF sleeves and disks. However, much of the art of handling this fragile material is not fully communicated in these procedures. To capture this art, a digital video of each step in fabrication and qualification is being made. A comprehensive video record will be completed in FY 2001 to serve as an archive of best practices and a back-up to the few skilled in the art.

2.2 IRIDIUM-ALLOY BLANK AND FOIL PRODUCTION

The goals for this activity are to produce flight-quality blanks and foil under full configuration control and to supply materials needed for clad vent set demonstration and maintenance activities. During the second quarter of FY 2000, iridium powder processing and electron beam melting of Ir-0.3% W was performed for the G3 ingot, and 69 blanks from 10 sheets from the G2 ingot were machined.

2.2.1 Blank Fabrication from G2 Ingot

Rolling was completed for the 11 sheets remaining from the 17 sheets from the G2 ingot. One of the sheets split longitudinally during a final bare rolling pass and will not yield blanks. A total of 69 blanks were electrodischarge machined from the ten rolled sheets. The 34 blanks from 5 of the sheets were surface ground and dimensionally inspected. A new inspector was trained in the requirements of the inspection procedure. A total of 32 passed the dimensional inspection. One blank was rejected for specified minimum diameter which was caused by slippage of the blank in the holder during electrodischarge machining and one blank did not clean up during grinding.

Courtesy thickness inspections were performed on all blanks in the region between 2 and 5 mm from the edge to determine the minimum thickness. The region within 5 mm from the edge of the blank has never been subjected to thickness measurement in the inspection procedure. Two additional blanks that meet requirements of the current inspection procedure exhibited a minimum thickness in this region less than 0.63 mm drawing requirement. The minimum measured thickness value was 062 mm for one blank and 0.61 mm for another. These regions were localized to a few mm. It is judged that these blanks are most likely to produce acceptable cups. Similar thickness data will be obtained for blanks ground in the future, to determine if any change in the thickness inspection procedure is justified. The 10 sheets are planned to produce 40 blanks during FY 2000 and additional blanks during FY 2001.

2.2.2 Blank Fabrication from G3 Ingot

Powder processing was continued for the G3 ingot using 17.4 kg of blended iridium powder. The processing, including blending with tungsten powder, compacting, sintering and electron beam melting was completed for four of the total of six batch blends for the G3 ingot. The G3 ingot is planned to yield 90 blanks during FY 2001.

2.2.3 Preparation of Scrap Iridium Ingot

Preparation of an iridium alloy scrap electrode, RS14, was completed. The starting material consisted of 11.5 kg of RS13 scrap ingot and other clean scrap which was not suitable for recycle into a flight-quality ingot, due to excessive impurity content or lack of traceability to iridium powder lots. The materials were arc-melted and drop-cast to produce 7 electrode segments with a total weight of 10 kg. The segments were electron-beam welded to produce and electrode 86 cm long. The electrode will be melted to verify proper equipment operation prior to melting of the G3 ingot.

The melting of this scrap will also serve to evaluate the use of a redesigned iridium pad. The modified pad, to which the arc is initially struck from the electrode at the bottom of the water-cooled copper mold, will be mechanically fixed to the bottom of the mold to prevent welding of the electrode to the pad. Welding of the pad to the electrode has occurred occasionally during the melting of iridium and other materials and requires that the melt be discontinued

immediately. A similar redesigned pad has been used for melting of a number of other materials in the same furnace with good success.

2.2.4 Testing of Blanks from AR2 Ingot

Blanks were previously machined from 4 sheets from the AR2 ingot, which were rolled without the use of molybdenum covers using a special instruction deviation request (SIDR). Tensile impact test results on this material showed tensile impact ductility values significantly lower than that for the AR2 material rolled with covers and significantly lower than the average of all Cassini production materials. Microstructural examination of the test samples was preformed and no obvious differences in microstructure were observed between high ductility and lower ductility samples or between the samples which were bare rolled and those rolled using the standard procedure. Some additional tests will be performed in the next quarter to rule out the possibility of inadequate specimen preparation for the tests in question.

2.3 CLAD VENT SETS AND WELD SHIELD

The goal of this activity is to produce flight quality (FQ) CVS and weld shields (WS) for inventory, test hardware and to maintain the production capability.

2.3.1 Qualification Production Status

Nine FQ and 5 Engineering Use (EU) matched assemblies were successfully matched, inspected, and packed to complete Qualification Production.

The Oak Ridge National Laboratory Process Evaluation Board (PEB) for CVS/WS Manufacturing met a number of times with the CVS/WS Manufacturing Operation Team during the last quarter of FY 1999. The Operation Team received a variety of action items that had to be completed before the PEB recommended release for unlimited flight quality production. The most significant concern of the PEB involved the 64% yield for flight quality vent cup assemblies (VCAs). This yield was attributed to decontamination covers not being uniformly in intimate contact with the vent cup during electron beam welding. This tended to produce areas with incomplete fusion from burnback of the (0.127 mm) 0.005-in.-thick decontamination cover.

The PEB also was concerned that only two non-flight quality VCAs had been evaluated using the solution (decontamination covers formed from compressed or flattened blanks) to the decontamination cover-to-cup welding problem. In light of these concerns 12 additional non-flight quality VCAs (9 scrap VCAs and 3 EU Qualification Production VCAs discussed below) were successfully welded with the new decontamination covers.

Five Qualification Production VCAs became EU units for a number of reasons. One VCA, 9753-30-A5NG, was found to have a small area with grain boundary separation near the center of the frit vent-to-cup weld. Also, this unit was used for a technical surveillance to evaluate the closure weld zone region via scanning electron microscopy and energy dispersive X-ray spectroscopy analysis (SEM/EDS). Additionally, a black spotted area on the bottom of the inner contour of the cup was found to contain several alumina-rich particles up to 200 μm in diameter. After the SEM/EDS analyses the particles were removed (based on visual observation at 30X magnification) by scraping them loose with a sharpened tungsten rod.

A second reweld was done for the decontamination cover-to-cup welds on VCAs 9753-30-4000, -4002, and -A5N8. Unfortunately, the areas in need of weld repair were toward the inner contour of the weld and the tantalum hold-down tips were lightly bonded to each decontamination cover. The decontamination covers were removed from each VCA. Next, the VCAs were straightened and the residual decontamination cover weld metal was removed by setting up each in a collet and grinding with a dish diamond grinding wheel (used for cup grinding-to-length operation) to bare clean-up. The minimum wall thicknesses were measured to be 0.596, 0.559, and 0.610 mm for VCA's 9753-30-4000, -4002, and -A5N8, respectively. The identity was re-scribed on each VCA. Finally, non-flight quality decontamination covers

made per the latest fabrication procedure (GPHS-XF-3619, Rev. J which calls for blanking, compressing or flattening, and then forming) were welded successfully to each VCA.

A second reweld was completed for the decontamination cover-to-cup weld on VCA 9753-30-A5NF but, unfortunately, it could only be successfully completed by rewelding without the use of the tantalum hold-down tip. This was because the area that needed to be rewelded was toward the inner contour of the weld and the tantalum tip would have prevented a complete repair and/or it would have been bonded to the decontamination cover (see above). Rewelding without the decontamination cover hold-down tip and moving the electron beam inward means that the weld and heat affected zone potentially are much closer to and possibly intersecting those of the frit vent-to-cup weld. Therefore, the VCA was downgraded for use as an EU unit.

On Monday December 20, 1999, the PEB and the Operations Team convened for a final review of the CVS/WS Manufacturing Demonstration effort. The PEB recommended that release be given for unlimited flight-quality production. Next, the Manufacturing Operation Team met on January 20, 2000, with a team appointed by the Department of Energy's Office of Space and Defense Power Systems for a review of the CVS Manufacturing Demonstration effort. The DOE-appointed team recommended that release be given for unlimited flight-quality production as directed in the future by the Office of Space and Defense Power Systems. Subsequently, an approval letter for future production of flight quality Clad Vent Sets (CVS) and Weld Shields (WS) was received from the Department of Energy's Office of Space and Defense Power Systems. This letter directs the Oak Ridge National Laboratory to: (1) implement the Galileo-type integral weld shield (IWS) for future CVS hardware production; (2) modify the 59 flight quality and 9 engineering use shield cups returned from Los Alamos National Laboratory (LANL); and (3) evaluate the effect(s) of the IWS and various combinations of vent notch widths on the girth weld process.

2.3.2 Training

One machinist has been trained for dimensional inspection. Plans have been made to train a second machinist as a dimensional inspector. This is being done to replace two inspectors who retired at the end of CY 1999. Eighty hours of hands-on inspection training for each machinist is required by the ORNL Plant and Equipment Division before official inspections can be done. Specific CVS/WS inspection training is being performed using previously inspected hardware consisting of 2 weld shields, 2 decontamination covers, 2 cover discs, 2 backing discs, 1 matched assembly, 1 vent cup assembly, and 1 shield cup. These results also were used for reinspection surveillance work.

The primary person responsible for processing frit vent assemblies (FVAs) and forming cups retired at the end of CY 1999. The primary person responsible for fabricating all foil components is being trained also for processing FVAs. So far, forty five FVAs have been processed as part of a combined training effort and furnace vacuum level evaluation (see sect. 2.3.5). The primary person responsible for cleaning all parts and packing for shipment is being trained also for forming cups. Eleven non-FQ blanks are being formed for this training.

2.3.3 Surveillances

Five CVS manufacturing technical surveillances were conducted. The first evaluated the vacuum furnace performance status. The second addressed profilometry used to measure roughness of the grit-blasted cups. The third dealt with ensuring that the flow rate equipment and standard are in good condition. The fourth surveillance assessed the reliability of the CVS manufacturing inspection processes through reinspections. The last one evaluated the procurement quality program. No deficiencies or corrective actions were identified during these surveillances. All items were found to be in good working order and reliable.

2.3.4 Decontamination Cover Blanking Optimization

The flattening operation, which was added to the decontamination cover fabrication process after blanking (prior to forming) to aid the decontamination cover-to-cup electron beam welding operation, increased the decontamination cover

diameters to near the upper limit. Therefore, different decontamination cover blanking-punch and die diameters were evaluated to determine the best tooling diameters for producing parts with diameters at split-tolerance. The finished part diameter (prior to welding) is required to be 11.5 to 11.6 mm, therefore, split-tolerance is 11.55 mm.

A blanking punch diameter of 11.610 mm (0.4571 in.) with a die diameter of 11.621 mm (0.4575 in.) yielded the best results. The diameters of seven parts were measured after blanking and flattening. They ranged from 11.628 to 11.662 mm. Thus, the flattened blank diameters ranged from 0.007 to .041 mm larger than the blanking die diameter. The variability in the increase is thought to be related to the anisotropy in the iridium foil and the inspection technique. The average ± 1 standard deviation for the low diameter measurements were 11.638 ± 0.006 mm while those for the high measurements were 11.655 ± 0.007 mm.

Forming of the decontamination cover tends to decrease its outer diameter. The actual as-formed part diameters for the seven parts measured as blanks ranged from 11.540 to 11.574 mm. The as-formed part diameters ranged from 0.066 to 0.108 mm smaller than the flattened blank diameters. Again, variability in the decrease is because of the anisotropy in the iridium foil and the inspection technique. A total of 13 parts have been formed after being blanked with the new tooling and flattened. The average ± 1 standard deviation for the low diameter measurements were 11.541 ± 0.009 mm while those for the high measurements were 11.558 ± 0.009 mm. The as-formed part diameters are very close to the split-tolerance, and no further work is planned to get them any closer. The blanking and forming tooling drawings and the procedure have been modified accordingly. The changes (DR-CVS-012) were submitted to and accepted by the Oak Ridge National Laboratory Iridium-Alloy Hardware Configuration Control Board.

2.3.5 Evaluation of High Temperature Vacuum Furnace with Graphite Hot Zone for Frit Vent Manufacturing

Three additional runs to 1900°C were made with four sets of tooling in the high temperature vacuum furnace A (ORNL property number X187885) with the retrofitted graphite hot zone to determine if the furnace was capable of meeting the 1 x 10^{-4} Torr maximum pressure requirement during the 1500°C sintering and 1900°C diffusion bonding operations. The ramp-up rate for the first run was changed from 15°C/min to 5°C/min. The second run was done using a ramp-up rate of 3°C/min while the third run used a 3°C/min ramp-up rate and a 1 h hold at 1250°C. The best performance occurred with the third run, however, the pressure peaked at an unacceptable (per present procedure) reading of 2.8 x 10^{-4} torr at the start of the 1900°C soak. The pressure only came down to 1.6 x 10^{-4} torr at the end of the 2 h soak.

It was decided that the most practical solution for meeting the procedural vacuum requirement would be to relax the requirement to 1 x 10^{-3} torr. Forty five frit vent assemblies have been processed so far as part of a combined training effort and vacuum level evaluation. The ramp-up rates have been increased to 20°C/min and 25°C/min for sintering and diffusion bonding to increase the pressure to as close as possible to the proposed 1 x 10^{-3} torr limit.

The bonding integrity of some of these frit vent assemblies will be evaluated metallographically and manually to get a qualitative sense of bond strength. The frit vent certification requirements of thickness and flow rate are being measured as well. Also, modeling of the sintering and diffusion bonding processes (which employ graphite tooling) is being done to make sure there are no significant differences in thermodynamic conditions at chamber pressure levels of 1x10^{-5}, 1x10^{-4}, and 1x10^{-3} torr in tungsten/molybdenum and graphite hot zones. If all of these evaluations show acceptable results, then a deviation request will be written to change the procedure to allow the higher pressure level.

2.4 IRIDIUM POWDER AND INVENTORY MANAGEMENT

The purpose of this work is to manage an iridium inventory for all heat source contractors with emphasis on the significant quantities of iridium located at Mound Plant, Los Alamos National Laboratory (LANL), and Oak Ridge National Laboratory (ORNL), and to maintain a no-change iridium inventory through an annual write-off of inventory and processing losses.

2.4.1 Iridium Accountability Review

A review at ORNL was performed on March 7, 8, and 9, 2000. The purpose of this review was to evaluate the accountability, physical inventory, and security of iridium. It was concluded that the accountability for the iridium was in place and operating in a proper manner. No recommendations were necessary.

2.5 SHIELD CUP MODIFICATION

The goal of this activity is to widen the vent notches and install the integral weld shield (IWS) in 59 FQ and 9 EU shield cups returned from Los Alamos National Laboratory (LANL).

2.5.1 Establishing Capability for Installing IWS

Preparations are underway for incorporating the IWS into shield cups. The IWS tooling that was used for early Cassini production was discarded after 1992 when the program shifted to the Type II weld shield. Five new pieces of tooling were fabricated to the latest design drawings. During initial tooling evaluation it became apparent that most of the drawings did not reflect the proper configuration. [Note: none of the tooling during early Cassini production was formally under configuration control.] Four out of the five Cassini-production tooling drawings and, therefore, the tooling recently produced to them were incorrect. The drawings and the tooling are being modified to meet product requirements. Procedures for the IWS, originally developed for the Cassini mission, are being reviewed and revised as necessary.

The vent notches in the shield cups returned from LANL will be modified under the existing Special Instruction Deviation Request (SIDR), SIDR-CVS-002. A new SIDR will be written for the IWS assembly process. Early shield cups processed per the new SIDR will be used to evaluate the effect(s) of the IWS and various combinations of vent notch widths on the girth weld process.

2.5.2 Vent Notch Widening of LANL Returns

Seven scrap cups were used to select the proper grinding wheel and establish the setup for the vent notch widening operation for the shield cups returned from LANL. Vent notches were widened on four additional scrap cups using the selected wheel and established setup. The widened vent notch depth x width measurements (in millimeters) were as follows: 3624-NC-0011, 0.178 x 0.602; 3625-25-2476, 0.186 x 0.514; 3625-25-2435, 0.164 x 0.518; and 3625-25-2491, 0.188 x 0.568. The drawing requirements are 0.15/0.20 mm for depth and 0.45/0.60 mm for width. Thus, 1 vent notch out of 4 on the scrap cups was nonconforming, which means the yield was 75%. This is consistent with the Cassini production experience of 13 nonconforming out of 60 widened vent notches, which amounted to a 78% yield. It should be pointed out that the 13 nonconforming widths during Cassini production ranged from 0.434 to 0.658 mm, and they were all accepted by the Material Review Board for flight quality use.

The vent notches on the 9 Engineering Use (EU) shield cups returned from LANL have been widened and courtesy inspected per Special Instruction Deviation Request (SIDR), SIDR-CVS-002. One vent notch (0.612 mm wide) exceeds the 0.60 mm maximum width while all the others meet the width and depth requirements. Two of these EU cups, 3625-25-2326 and -2339, were given courtesy full dimensional inspections. These inspections indicated that the cup outside radii were larger than the 5.68/5.96 mm requirement. Follow-up radii measurements were made using different inspection techniques (standard optical comparator, toolmaker's microscope, and coordinate measuring machine [CMM]). These measurements confirmed the initial out-of-tolerance results, however, they also showed that the CMM results were significantly more repeatable. In light of this a deviation request (DR-CVS-014) will be written to change the radius certification inspection technique from optical comparator to the CMM.

All 9 EU cups were dye penetrant inspected. Indications were noted only on the inside sidewall of all but two of the cups. These cups were produced in 1991 and 1992 during early Cassini production with the integral weld shields

welded inside. In 1994 the cups were returned from LANL to have the IWS removed and the vent notches widened. When the weld shields were removed, the tab weld areas were reworked to the minimum wall thickness permissible. However, subsequent dye penetrant inspection showed indications in some of these areas for all of these cups. This was deemed acceptable for the EU applications intended for these cups. The indications recently found on the inside sidewalls correspond to those found and documented previously in 1994. No new indications were found. Thus, the cups are acceptable from the dye penetrant inspection standpoint. Now the cups are being dimensionally inspected for cup certification. Next, the cups will be cleaned, given an air burn-off, and vacuum outgassed in preparation for installing new IWS. Concurrently, the vent notches have been widened for the 59 flight quality cups. These cups are currently being dye-penetrant inspected.

3. BASE TECHNOLOGY PROGRAM AND TECHNICAL SUPPORT ACTIVITIES

3.1 TECHNICAL SUPPORT FOR ARPS AMTEC CELL DEVELOPMENT

3.1.1 Introduction

The AMTEC cell is one of the primary thermal to electric conversion technologies being considered for future NASA outer planetary space missions. These cells use refractory metal alloys as materials of construction and sodium (Na) as a working fluid. ORNL is providing technical support to the AMTEC development program by providing materials fabrication, mechanical property data support, and component joining fabrication with the electron beam (EB) welding process. Nb-1Zr has been the primary material for the cell components developed for the ARPS Program. Oxidation concerns with this alloy have lead to the study of Mo-41Re as an alternate material. Mo-Re alloy sheet is being produced for evaluation in AMTEC development cells. Oxidation studies are being conducted on materials for the AMTEC application.

3.1.2 Oxidation Studies

Studies of the oxidation behavior of Mo-41Re are being carried out in vacuum and argon, and weight change results are summarized in Table 3.1. At 400 and 500°C, weight changes were minimal after 500 h exposures in vacuum containing 1×10^{-4} torr oxygen. At 400°C, the surface appearance of the samples was unchanged from that of the before exposure samples, a further indication of a lack of reaction. At 600°C, there was a significant, but not large, weight loss after 504 h at 1×10^{-4} torr oxygen. Weight losses are usually associated with evaporation of MoO_3. At 900°C, small weight gains were recorded after 500 h at 1×10^{-6} torr oxygen. Weight gains are usually associated with formation of MoO_2. High temperatures and high partial pressures of P_O generally favor formation of MoO_3. However, in the above tests at 900°C, pressure of oxygen was much lower at 900°C versus the 600°C tests and it would appear that the lower pressure suppressed formation of MoO_3.

Room temperature tensile tests of selected samples after oxidation have been conducted as shown in Table 3.2. As previously indicated, there is no systematic decline in strength or ductility of Mo-41Re as a function of oxidation temperature, time or weight change. Weight increases >10,000 ppm were measured without significantly lowering the ductility of Mo-41%Re compared with other as-oxidized samples. However, before test material (M-12) was both stronger and more ductile than any of the as-oxidized samples. The before-test sample had been annealed at 1400°C and recrystallization was confirmed by metallography. If oxidation resulted in an increase in dissolved oxygen, the sample strength should have increased not decreased. The reason for this type of change remains unexplained.

3.1.3 AMTEC Cell Fabrication Development

The EPX-01-E3 cell assembly was initiated and welded during this reporting period. Two anomalies occurred while welding the BASE tube flanges to the BASE support plate. The first was the appearance of cracking in the Nb-1Zr Base plate at the weld joint area while preheating the component. It was learned that TiNi braze alloy had been used to join the sapphire insulator to the BASE tube flanges. This had apparently melted and caused localized cracking. It did not

Table 3.1. Oxidation of Mo-41Re in vacuum and argon

Sample number	Temperature (°C)	P_O (torr)	Time (h)	Weight change (mg)	Weight change (mg/cm^2)	Weight change ($mg/cm^2/h$)	Weight change (ppm)	Surface appearance (color)
M-27	400	1×10^{-4}	100	-.02	-.01	-1×10^{-4}	-40	Metallic (no change)
M-28	400	1×10^{-4}	100	-.02	-.01	-1×10^{-4}	-40	Metallic(no change)
M-35	500	1×10^{-4}	250	+.01	+.005	$+2 \times 10^{-5}$	+20	Gold-to-copper/gold
M-36	500	1×10^{-4}	250	-.01	-.005	-2×10^{-5}	-20	Gold-to-copper/gold
M-29	500	1×10^{-4}	500	-.08	-.04	-8×10^{-5}	-157	Copper-gold
M-30	500	1×10^{-4}	500	-.02	-.01	-2×10^{-5}	-40	Copper-gold
M-31	600	1×10^{-4}	504	-.11	-.055	-1×10^{-4}	-218	Brownish purple
M-32	600	1×10^{-4}	504	-.16	-.08	-1.6×10^{-4}	-322	Brownish purple
M-33	900	1×10^{-6}	500	-.26	+.13	$+2.6 \times 10^{-4}$	+519	Brown
M-34	900	1×10^{-6}	500	-.24	+.12	$+2.4 \times 10^{-4}$	+472	Brown
				Argon (1 atm)				
M-21	900	3×10^{-3}	100	+.16	+.08	$+8 \times 10^{-4}$	+322	Brown
M-22	900	3×10^{-3}	100	+.15	+.075	$+7.5 \times 10^{-4}$	+310	Brown
M-25	900	3×10^{-3}	500	+1.97	+.99	$+2 \times 10^{-3}$	+3,883	Brown
M-26	900	3×10^{-3}	500	+2.04	+1.02	$+2 \times 10^{-3}$	+4,106	Brown
M-23	900	3×10^{-3}	1,000	+5.48	+2.74	$+2.7 \times 10^{-3}$	+10,861	Brownish-purple
M-24	900	3×10^{-3}	1,000	+5.28	+2.64	$+2.7 \times 10^{-3}$	+10,504	Brownish-purple

Table 3.2. Room temperature tensile properties of Mo-41Re

Sample number	Oxidation temperature	P_{O_2} (torr)	Weight change (ppm)	YS (MPa)	UTS (MPa)	Uniform elongation (%)	Total elongation (%)
M-12	—	—	—	739	962	19	29
			Vacuum				
M-32	600	1×10^{-4}	-322	548	688	13	15
			Argon (1 atm)				
M-21	900	3×10^{-3}	+322	564	734	13	14
M-22	900	3×10^{-3}	+310	586	776	14	17
M-25	900	3×10^{-3}	+3,883	557	719	13	18
M-23	900	3×10^{-3}	+10,861	506	668	13	17

appear to have a seriously detrimental effect on the weld. The second problem was observed upon inspection at the completion of the BASE tube welds. Two of the eight sapphire insulators were cracked by the welding operation. Subsequent leak rate testing of the subassembly, however, revealed an acceptable leak rate. The cell assembly was completed and welded using the previously developed procedures. Leak testing of the completed assembly revealed two areas with leaks in the upper cell wall to cold end circumferential weld. The cell was returned to AMPS for further evaluation and repair. Repair welds were accomplished at AMPS by EB welding patches over the leak areas. Another leak was detected at the pump out port to cold cap weld after a brazing operation was performed. A glass seal was reportedly used to repair this leak.

Possible causes of these leaks have included contamination from vacuum grease, cutting fluids, and low ductility, coarse-grained microstructure in the cold end cap resulting from the high temperature brazing operation. Analyses are being performed at AMPS to understand and correct these problem areas.

Welding development tests were then conducted for various components of the AMTEC cell. These tests were necessary to select welding parameters for the electron beam welds for the latest design of the BASE tube support plate. BASE tube subassemblies were welded into the BASE support plate with various combinations of preheat temperature and welding power. These tests were conducted to assess the potential for cracking the sapphire insulators of the BASE tube subassemblies and evaluate weld penetration between the BASE tube flange and the BASE tube support plate. Welding parameters for the BASE tube support plugs and hot end cap were also developed. Weldments were sectioned and examined by optical metallography. Based on the results of these test, 350°C was selected as an acceptable preheat temperature since no cracking of the sapphire was observed in any of the weldments at this temperature. Welding parameters which produced uniform seal welds were established for the different joints. The new welding parameters were used to fabricate a second test subassembly prior to applying them to a complete test cell. Examination of this test subassembly showed no evidence of insulator cracking or welding concerns with the other weldments.

Assembly and welding of the EPX-01E4 cell were completed during this reporting period. A problem was encountered with the upper cell wall to center rib weld. A fit up problem was found between these two components during assembly. It was judged by the AMPS personnel to be acceptable for welding after some adjustments were made to the components. Electron beam welding of this joint resulted in a hole which could not be repaired by welding. The rib and cell wall in this area were reported to be thin. The remainder of the cell joints was welded and it was planned to attempt a repair of the hole by brazing a patch at AMPS. Digital radiography was performed on the cell to characterize the internal configuration of components.

3.1.4 Molybdenum-41% Rhenium Alloy Sheet and Foil Production

The goals for this activity are to produce arc-melted Mo-41%Re sheet for AMTEC demonstration cells. During the second quarter of FY 2000, a molybdenum can was prepared with a thermocouple well to permit direct measurement of the billet temperature in order to calibrate the induction billet heater for extrusion of Mo-Re billets inside an evacuated molybdenum can. It is anticipated that this will reduce the surface cracking observed in the previous two extrusions of Mo-41%Re. The MR3 ingot, of about 10 kg, will be extruded within the same can and rolled to produce plate materials for developmental cells. Sections of the MR2 extrusion have been hot rolled to 10 mm and 7 mm (0.40 and 0.30 in.) thickness respectively to provide material for a hot end support plates and center wall ribs for a cell. Machining of components from Mo-41%Re alloy plate to produce one AMTEC mock-up cell was initiated. One lower cell wall weld ring, one hot end cap plug, and eight base tube hole plugs were machined. One component of each of the middle cell wall rib, cold end top cap, and hot end support plate is planned for April. In addition Mo-41% Re sheet, 0.5 mm thick by 7 cm wide by 30 cm long, was recrystallized at 1400°C and provided to Mound Plant for testing and evaluation.

3.2 ALLOY DEVELOPMENT AND CHARACTERIZATION

3.2.1 Oxygen Compatibility of Ce-doped Iridium Alloys at 1330 °C and an Oxygen Partial Pressure of 13.3 MPa

Considerable progress has been made in our alloy design effort to develop an alloy with a lower thorium addition than that in DOP-26. In 1995, an alloy containing 29 ppm Ce and 18 ppm Th was chosen for scale up and was designated as DOP-Ce or DOP-40 (ref. 1). Compared to DOP-26, this alloy has been shown to have better weldability, comparable impact ductility, and comparable grain growth in vacuum.[2-5] Because it is also desirable to know the grain growth characteristics of this alloy in low pressures of oxygen, as soon as specimens were available, they were included in our oxygen compatibility tests.

Over the past seven years, low-pressure oxygen compatibility tests have been conducted on several DOP-26 iridium alloys from both the old and new fabrication processes.[6-12] The conditions of each test, the alloys included in each test, and the dates of the final reports are shown in Table 3.3. The old-process ZR and new-process D2 materials were tested at all six conditions listed, and the results of those tests indicate that there is no significant difference in grain growth behavior between the old- and new-process alloys. Various Ce-doped alloys have also been included over the years as the development of the Ce-doped alloy progressed. Specimens of DOP-40 (I1 ingot) have been included in the three series of tests at the 13.3 mPa oxygen level.[9-11] Earlier tests at an oxygen level of 1.3 mPa (refs. 6-8) have included various Ce-doped experimental alloys whose compositions are shown in Table 3.3. Recent impact test results indicate that DOP-40 alloys containing 20 to 40 ppm Ce and 30 to 50 ppm Th have as good or better impact ductilities than currently used DOP-26 iridium over the entire temperature range tested (800-1300°C) (ref. 5). Therefore, information on the oxygen compatibility of these alloys is needed.

The purpose of this report is to present data obtained for DOP-40 alloys containing 20 to 40 ppm Ce and 30 to 50 ppm Th tested at 1330°C using the higher oxygen partial pressure (10^{-4} torr, 13.3 mPa) and to compare the results with those from previous tests from both Ce-doped alloys and DOP-26. These alloys have been included in the oxygen compatibility studies to determine whether cerium, which has been found to segregate to grain boundaries and form Ir_5Ce precipitates in iridium alloys,[13,14] will leave the grain boundaries and diffuse to free surfaces to form cerium oxide (similar to the behavior of thorium). As with thorium, the diffusion of cerium from the grain boundaries and the dissolution of Ir_5Ce precipitates would result in the unpinning of the grain boundaries causing anomalous surface grain growth and reduced impact ductility.[15,16]

Table 3.3. Description of DOP-26 and Ce-doped iridium alloys tested in low pressures of oxygen and references to results

Oxygen Pressure (mPa)	Temperature (°C)	DOP-26[a] (old process)	DOP-26[a] (new process)	Ce-doped[a]	Date of report to DOE [ref.]
1.3	1330	ZR	D2,E2	Ce-2	4/24/92 [6]
	1280	ZR	D2,E2	Ce-3	6/25/93 [7]
	1230	ZR	D2,E2	Ce-3, E-815	8/29/94 [8]
13.3	1330	ZR	D2,E2	I1	2/25/97 [9]
	1280	ZR,B706	D2	I1	3/27/98 [10]
	1230	ZR,B706	D2	I1, I-103	2/26/99 [11]

[a]ZR, D2, E2 = 60 ppm Th; Ce-2 = 60 ppm Th + 36 ppm Ce; Ce-3 (E-809) = 50 ppm Ce; E-815 = 20 ppm Th + 30 ppm Ce; DOP-40 (I1) = 18 ppm Th + 29 ppm Ce; I-103 = 30 ppm Th + 30 ppm Ce

In this series of tests, specimens were cut from DOP-40 ingots denoted as I-102, 103, 104, and 105 with Ce/Th compositions as listed in Table 3.4. These ingots were fabricated from 500-g heats using the old process.[12] Also included in this series of tests were specimens of the D2 ingot, fabricated by the new process. Since previous testing has shown that there is no significant difference in the oxygen compatibility of old and new-process DOP-26, the D2 specimens were used as controls in this series of tests.

Table 3.4. Nominal dopant levels of DOP-40 (Ir-0.3%W) alloys

Alloy No.	Ce (wppm)	Th (wppm)
I-102	20	40
I-103	30	30
I-104	30	40
I-105	30	50

All Ce/Th-doped samples used in this study were cut from rolled sheets and the D2 samples were cut from a fabricated "blank." The samples were recrystallized for 1 h at 1375°C in vacuum (10^{-4} Pa range) prior to oxygen annealing. Oxygen annealing was performed at 1330°C in a dynamically pumped tube furnace having a base pressure of 4×10^{-4} Pa (3×10^{-6} torr). An oxygen leak valve, upstream from the samples, was adjusted so that the ion gage pressure halfway between the leak valve and the samples was 1.3×10^{-2} Pa (13.3 mPa). The samples were hung on iridium wires in such a way as to separate them and provide for uniform flow of oxygen to all surfaces of all samples. Since several different annealing times were used, a furnace entry system was used that allowed for easy entry and exit of samples without temperature cycling of the furnace. Samples were grouped according to the time of exposure that each group would receive, and all were placed in the furnace at the beginning of the test. After each allotted time (e.g., 1 week, 1 month, etc.), the furnace was opened and one group removed. The maximum exposure time of the oxygen anneals was approximately 3000 h (4 months).

Optical metallography techniques[12] of polishing, etching, and measuring grain sizes were used to determine the grain growth as a function of exposure time. Grain sizes were measured by the method of linear intercepts in both the short transverse (ST) and long transverse (LT) directions with respect to the rolling direction. Grain sizes were also measured in the LT direction as a function of depth into the specimen in order to determine the degree of anomalous growth of near-surface grains. The confidence limits of the data are indicated by the number of intercepts counted for each data point (recorded in parentheses in the tables).

Table 3.5 and Fig. 3.1 show the average grain size in both the ST and LT directions for DOP-40 heats I-102 through I-105 exposed for up to 3000 h at 1330°C in an oxygen partial pressure of 13.3 mPa. Data for the D2 (new process) DOP-26 heat are included for comparison. Although the DOP-40 alloys used in this study were prepared using the old fabrication process, their comparison to new process D2 material is justified since past studies of old- and new-process DOP-26 at 1230, 1280, and 1330°C in oxygen levels of 1.3 and 13.3 mPa have shown no difference in their oxygen compatibility[6-12]. Figure 3.1(a) shows that grain growth of all four Ce/Th-doped alloys is comparable to that of the D2 (new process) DOP-26 material in the ST direction. In Fig. 3.11(b), grain sizes for the Ce/Th-doped alloys are slightly higher than for the DOP-26 alloy. This result was previously noted for the I1 heat of DOP-40 (ref. 17). Within the deviations of the data, no difference in average grain size or grain growth behavior between the four Ce/Th-doped alloys was observed.

Table 3.5. Grain size of the Th/Ce-doped DOP-40 alloys as a function of exposure time at 1330°C and an oxygen partial pressure of 13.3 mPa

Alloy	Annealing time (h)	Grain size (μm)	
		ST direction	LT direction
D2	As Rxn [a]	22 (2255)	38 (2981)
	666	39.0 (1264)	53.6 (686)
	1502	43.4 (1178)	60.5 (602)
	2315	46.4 (1089)	64.6 (577)
	3000	50.9 (948)	68.7 (533)
I-102	As Rxn [a]	18.1 (2612)	45.0 (1152)
	330	31.6 (1619)	66.4 (563)
	666	36.7 (1393)	64.9 (575)
	1502	43.4 (1179)	83.3 (469)
	2315	48.2 (1248)	94.8 (424)
	3000	48.1 (1041)	88.5 (436)
I-103	As Rxn [a]	18.4 (1813)	45.1 (1154)
	330	34.4 (1374)	72.6 (533)
	666	38.8 (1210)	73.8 (431)
	1502	45.1 (1086)	81.1 (507)
	2315	53.3 (2600)	89.3 (348)
	3000	56.1 (859)	90.3 (345)
I-104	As Rxn [a]	17.0 (3013)	40.3 (1293)
	330	30.9 (1599)	68.6 (546)
	666	34.8 (1412)	69.7 (557)
	1502	42.6 (1149)	76.6 (493)
	2315	45.0 (1128)	86.7 (453)
	3000	49.3 (1028)	82.9 (460)
I-105	As Rxn [a]	18.5 (2715)	47.0 (1114)
	330	33.7 (1465)	67.8 (560)
	666	39.5 (1269)	73.6 (514)
	1502	46.0 (1117)	74.3 (498)
	2315	47.0 (1061)	86.0 (441)
	3000	50.2 (978)	80.0 (479)

[a]Without anneal.

(a)

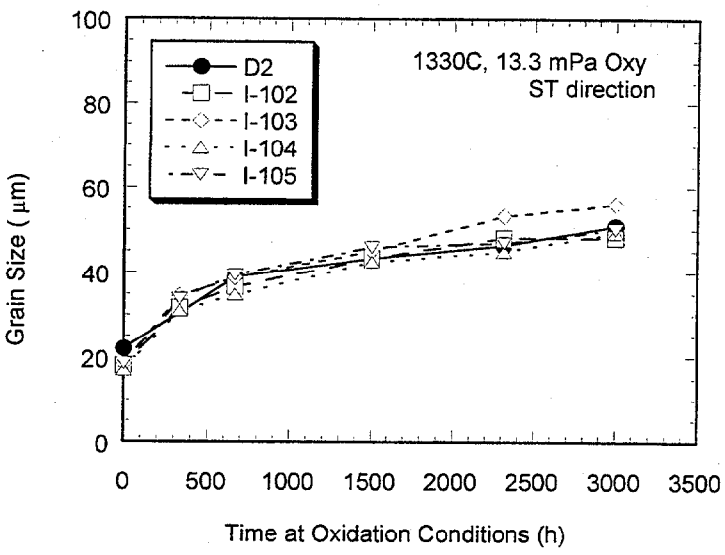

(b)

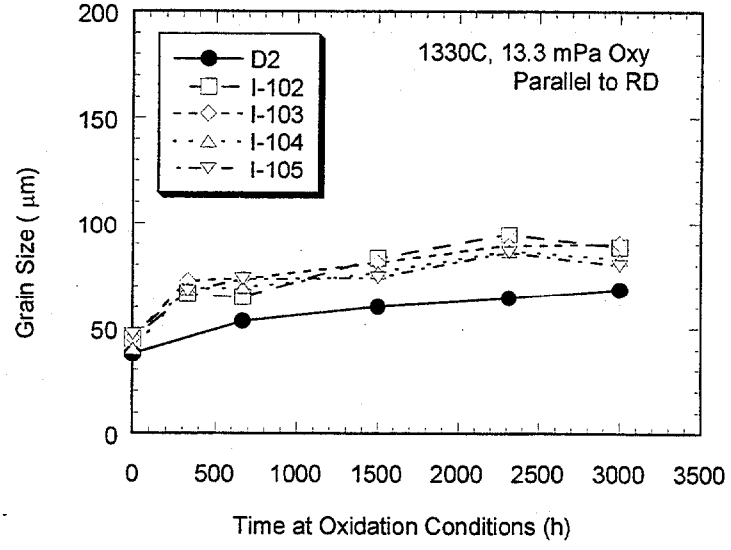

Fig. 3.1. Grain size as a function of time of exposure at 1330°C in an oxygen partial pressure of 13.3 mPa for four Ce/Th-doped DOP-40 alloys and the new-process DOP-26 D2 alloy in the (a) ST and (b) LT direction with respect to the rolling direction.

This is first time that alloys I-102, 104, and 105 have been tested. However, alloy I-103 was tested previously at 1230°C in 13.3 mPa oxygen [17]. Figure 3.2 compares the average grain sizes of alloy I-103 at both 1230 and 1330°C with data for the D2 DOP-26 (new process) alloy. In both cases the D2 samples were exposed at the same time as the I-103 samples. There was no difference in grain growth behavior for the two alloys in the ST direction [Fig. 3.2(a)]. However, in the LT direction [Fig. 3.2(b)], the Ce/Th-doped I-103 alloy had slightly higher grain sizes, especially in the tests conducted at 1330°C. The results are the same if the Ce/Th-doped I-103 alloy is compared against old-process DOP-26, as shown in Fig. 3.3.

In Fig. 3.4, the average grain sizes of the I-103 and D2 specimens from the current study are compared with data generated earlier at these same test conditions for old- (ZR) and new-process (D2) DOP-26 and the I1 ingot of DOP-40 (ref. 9). Again the data for the I-103 and DOP-26 alloys are comparable in the ST direction, while in the LT direction, the I-103 has slightly higher grain sizes. The I1 heat of DOP-40 has been tested at 1230, 1280, and 1330°C (all in 13.3 mPa oxygen) and has consistently shown slightly higher grain sizes than the DOP-26 material. In past reports (refs. 9,10,17) this difference has been described as being within the experimental deviations of the grain size measurements or due to the larger starting grain size of the I1 alloy. However, since the grain size data for the I-103 alloy is much closer to that of the DOP-26 material, the higher grain size of the I1 alloy may suggest a relationship between the amount of Th in the alloy and grain growth in oxygen. The I1 alloy contains 29 ppm Ce but only 18 ppm Th, while all the Ce/Th-doped alloys used in the present study contain 30-50 ppm Th. No difference in grain growth in vacuum has been noted for any of the DOP-40 heats compared to DOP-26 (2,4,18).

Table 3.6 and Figs. 3.5 through 3.9 show grain sizes in the LT direction as a function of depth into the specimen for the alloys used in this study. Plotting the grain size in this manner allows one to determine the tendency for anomalous growth of near-surface grains. More rapid growth of near-surface grains indicates that the Th and/or Ce are diffusing out of the material and are therefore unavailable for pinning of the grain boundaries[15,16]. The D2 DOP-26 alloy was previously tested at 1330°C in 13 mPa oxygen;[9] the current results for this alloy, shown in Fig. 3.5, are comparable to those reported previously. There was only minimal grain growth of surface grains in D2, with grain sizes remaining below approximately 90 μm even after 3000 h of exposure.

The four Ce/Th-doped alloys showed a higher tendency for anomalous grain growth of the near-surface grains in the LT direction compared to the D2 material. After 3000 h of exposure their near-surface (50-150 μm below the surface) grain sizes ranged from 100 to 120 μm (see Figs. 3.6-3.9). This is shown more clearly in Fig. 3.10 where the 0 and 3000 h grain sizes for the D2 DOP-26 alloy and the four Ce/Th-doped alloys are plotted as a function of depth below the surface. As noted previously,[17] a possible reason for the larger near-surface grain sizes in the Ce/Th-doped material is the smaller mass of Ce relative to Th which would result in faster diffusion. Within the deviations of the data, there does not appear to be any difference between the four Ce/Th-doped alloys in terms of their tendency for near-surface grain growth.

In summary, oxygen compatibility studies were conducted on specimens from the I-102 through I-105 ingots of DOP-40 at an oxygen partial pressure of 13.3 mPa and a temperature of 1330°C for times up to 3000 h. Specimens of the new-process D2 DOP-26 material were included for comparison purposes. In terms of average grain size and grain growth rates in the ST direction as a function of time, the DOP-40 alloys are comparable to DOP-26. In the LT direction, although the starting grain sizes of the DOP-40 alloys were comparable to that of the DOP-26 material, average grain sizes as a function of time are slightly larger for the Ce/Th-doped DOP-40 alloys. Initially, the Ce/Th-doped alloys may experience slightly higher grain growth rates than DOP-26 in the LT direction, but after about two weeks time the data indicates that the rates of grain growth are comparable for both materials. Comparison with earlier results (i.e., DOP-40 ingot I1) suggests that as long as the thorium level in DOP-40 is approximately 30 ppm, its grain growth behavior in low-pressure oxygen is similar to that of DOP-26.

Further testing of DOP-40 alloys containing a range of Ce and Th concentrations at other temperatures and oxygen partial pressures is planned.

(a)

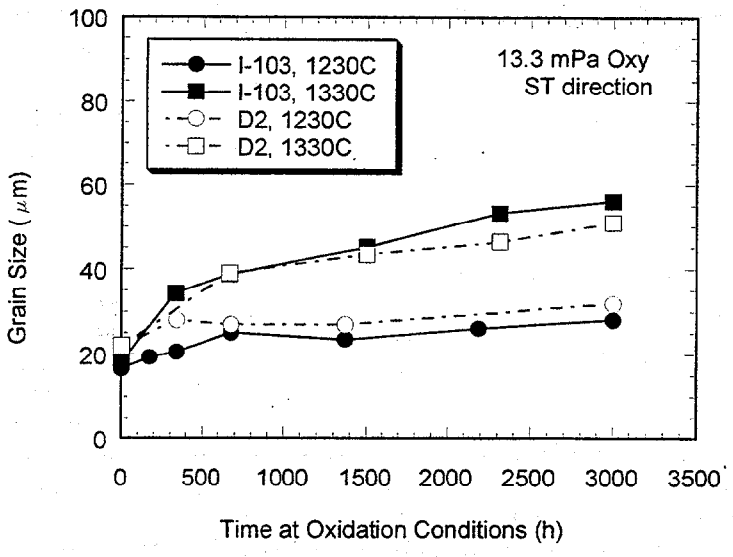

(b)

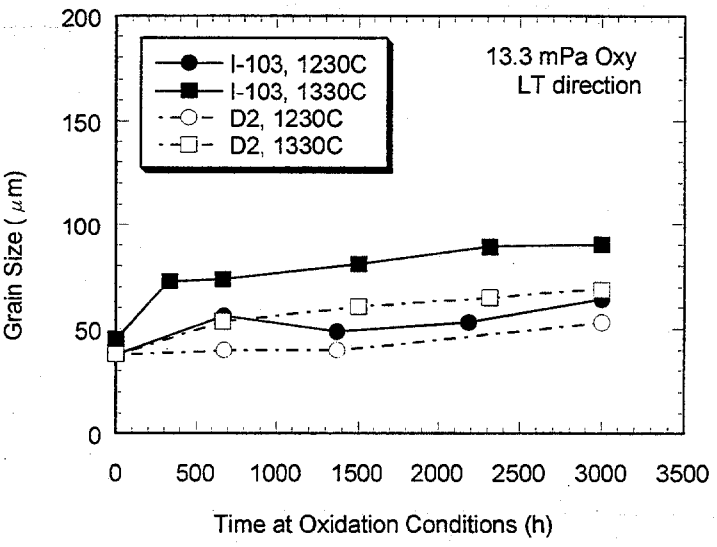

Fig. 3.2. Comparison of grain size as a function of time of exposure at two different temperatures in an oxygen partial pressure of 13.3 mPa for the Ce/Th-doped I-103 alloy and the new-process DOP-26 D2 alloy in the (a) ST and (b) LT direction with respect to the rolling direction. 1230°C data taken from ref. 11.

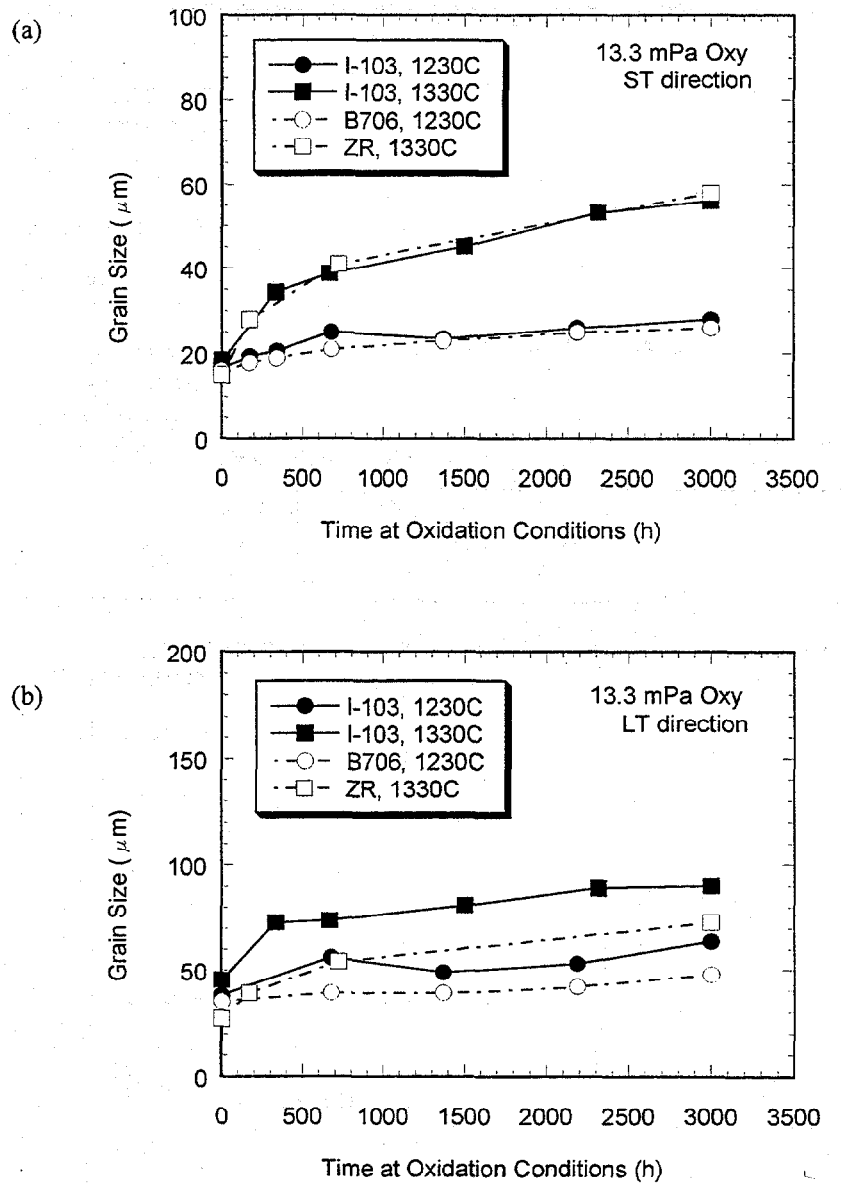

Fig. 3.3. Comparison of grain size as a function of time of exposure at two different temperatures in an oxygen partial pressure of 13.3 mPa for the Ce/Th-doped I-103 alloy and the old-process DOP-26 (ZR and B706) alloy in the (a) ST and (b) LT direction with respect to the rolling direction. 1230° data taken from Ref. 11; ZR,1330°C taken from ref. 9.

(a)

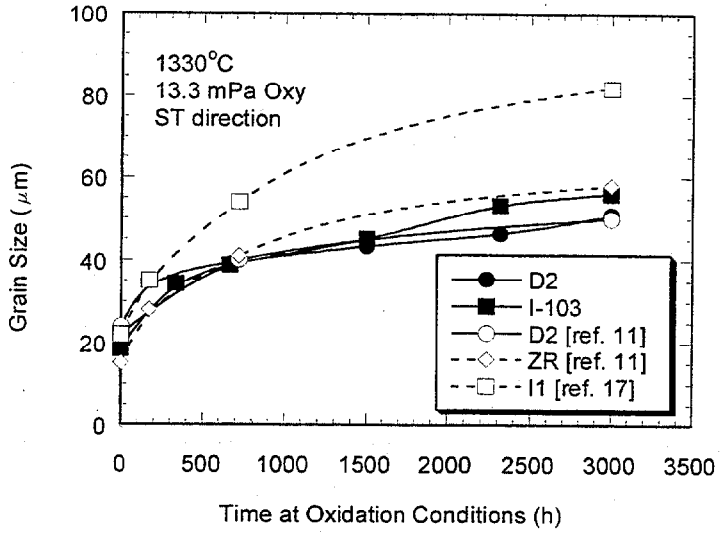

(b)

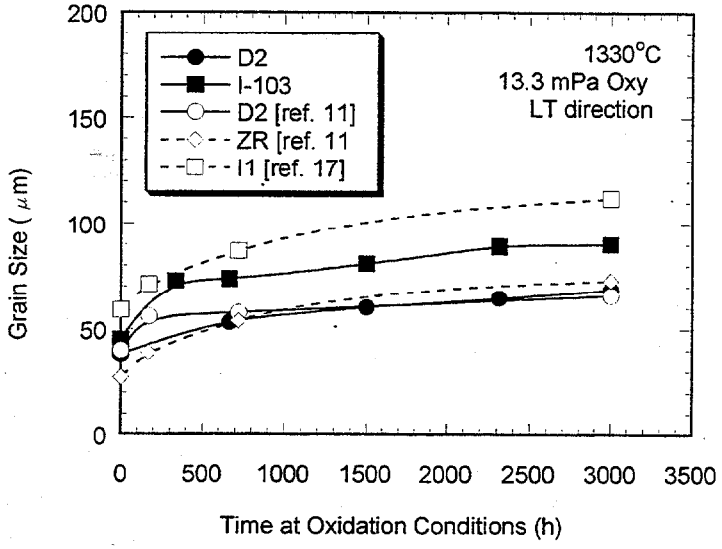

Fig. 3.4. Comparison of grain size as a function of time of exposure at 1330°C in an oxygen partial pressure of 13.3 mPa for the Ce/Th-doped I1 and I-103 alloys and both new- and old-process DOP-26 alloys in the (a) ST and (b) LT direction with respect to the rolling direction.

Table 3.6. Average grain size (μm) as a function of depth below the surface of the specimen for DOP-40 specimens exposed to an oxygen partial pressure of 13.3 mPa at 1330°C

Alloy	Exposure time (h)	Depth below surface (μm)					
		50	100	150	200	250	300
D2	0	51.8	48.1	46.5	44.6	47.2	42.7
	666	53.4	62.7	50.9	52.4	51.1	50.9
	1502	67.4	68.2	56.9	54.8	60.2	55.6
	2315	65.4	72.2	67.2	56.4	56.1	56.6
	3000	72.8	72.0	68.1	67.5	65.2	66.6
I-102	0	52.1	46.9	42.4	45.1	41.1	42.2
	330	69.2	68.6	60.2	67.6	68.1	64.5
	666	76.2	65.4	66.3	62.6	62.3	56.6
	1502	116.8	103.8	62.6	76.4	75.1	65.2
	2315	124.7	108.8	96.2	98.2	67.5	73.2
	3000	98.1	108.5	98.0	79.8	73.4	66.2
I-103	0	49.9	46.1	47.3	44.2	45.5	37.8
	330	83.2	77.8	75.6	66.6	72.6	59.7
	666	93.2	78.7	65.4	65.8	65.8	--
	1502	113.7	86.7	78.1	62.0	58.7	57.0
	2315	96.4	101.4	87.8	85.8	75.2	--
	3000	106.1	99.6	85.2	80.5	80.0	--
I-104	0	45.4	41.5	37.1	41.8	36.4	39.3
	330	73.0	61.9	76.3	57.3	69.6	73.1
	666	105.9	63.4	63.4	53.0	61.9	70.4
	1502	103.5	86.5	65.7	64.2	75.3	64.5
	2315	117.1	99.6	91.4	72.9	64.7	74.5
	3000	88.0	107.0	90.6	71.6	66.8	73.7
I-105	0	50.5	51.0	42.5	45.6	40.1	52.3
	330	67.7	69.4	75.5	68.9	66.4	58.7
	666	80.6	82.8	64.8	76.4	75.7	61.3
	1502	79.6	85.6	67.7	64.3	67.5	81.3
	2315	83.3	103.0	88.5	76.9	76.8	87.6
	3000	87.1	108.4	88.5	69.2	67.2	59.9

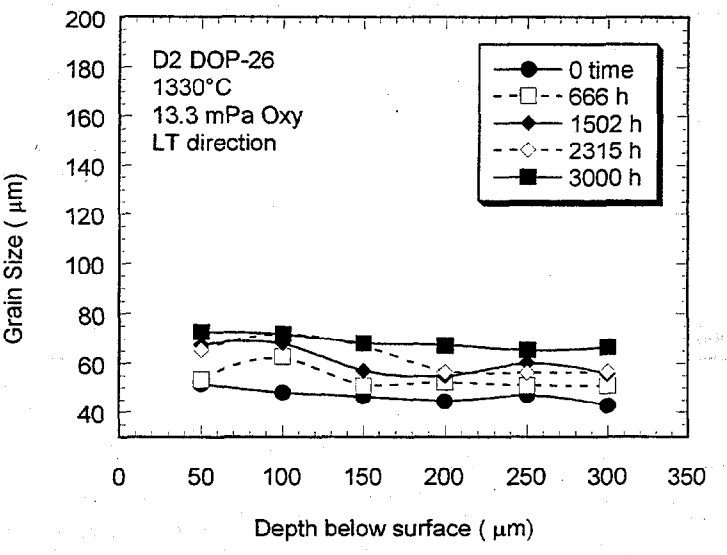

Fig. 3.5. Grain size in the LT direction as a function of depth below the surface of the sample and time of exposure for the D2 DOP-26 alloy annealed at 1330°C in an oxygen partial pressure of13.3 mPa.

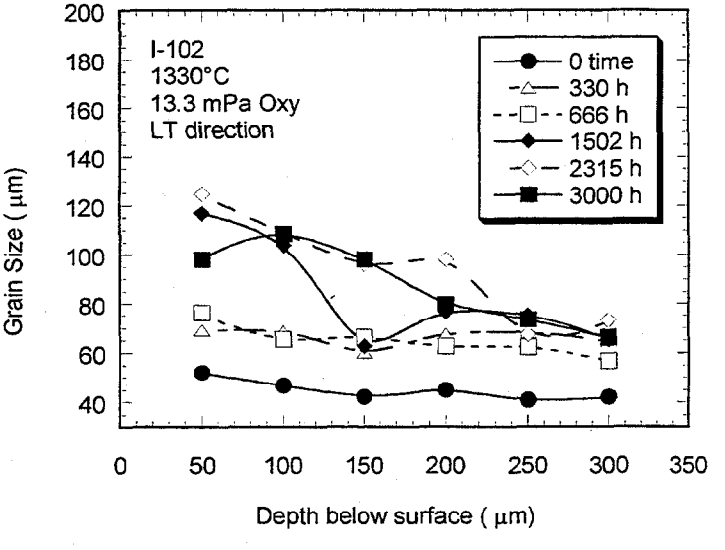

Fig. 3.6. Grain size in the LT direction as a function of depth below the surface of the sample and time of exposure for the Ce/Th-doped I-102 alloy annealed at 1330°C in an oxygen partial pressure of13.3 mPa.

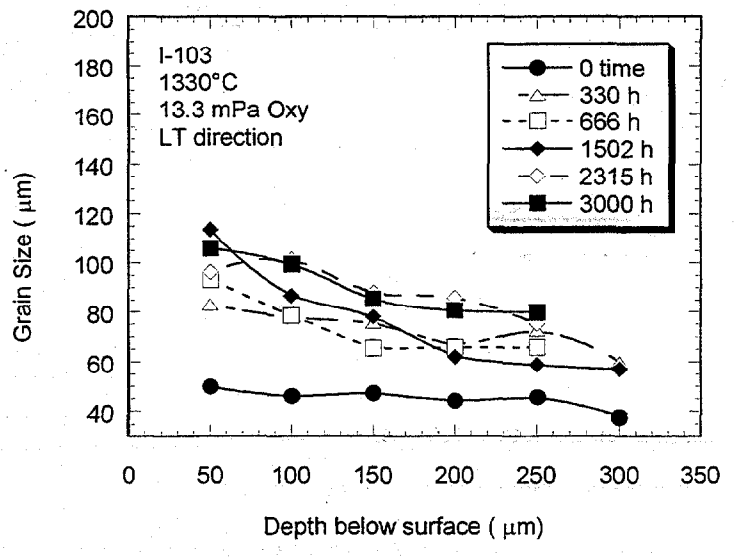

Fig. 3.7. Grain size in the LT direction as a function of depth below the surface of the sample and time of exposure for the Ce/Th-doped I-103 alloy annealed at 1330°C in an oxygen partial pressure of13.3 mPa.

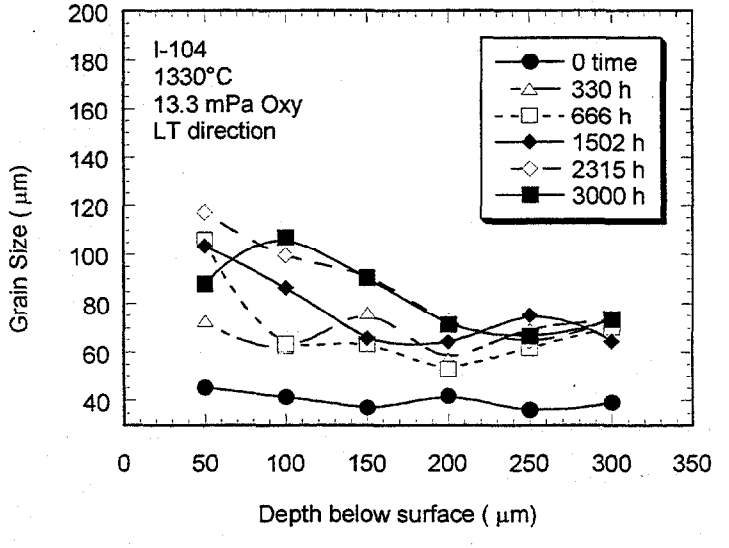

Fig. 3.8. Grain size in the LT direction as a function of depth below the surface of the sample and time of exposure for the Ce/Th-doped I-104 alloy annealed at 1330°C in an oxygen partial pressure of13.3 mPa.

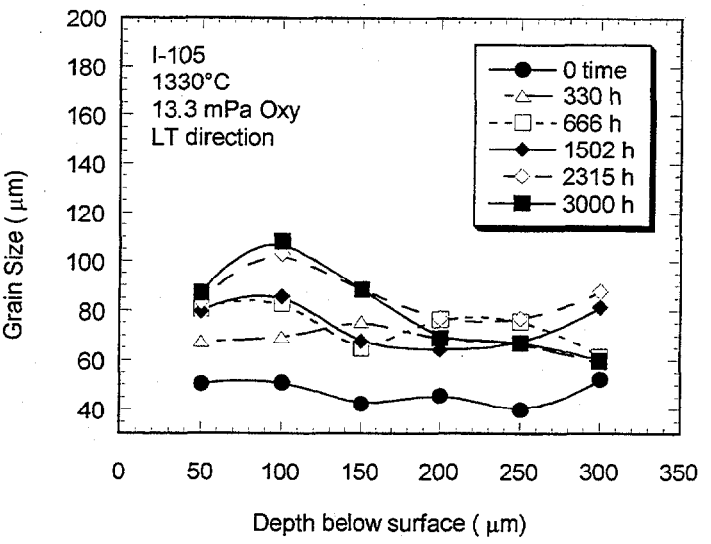

Fig. 3.9. Grain size in the LT direction as a function of depth below the surface of the sample and time of exposure for the Ce/Th-doped I-105 alloy annealed at 1330°C in an oxygen partial pressure of 13.3 mPa.

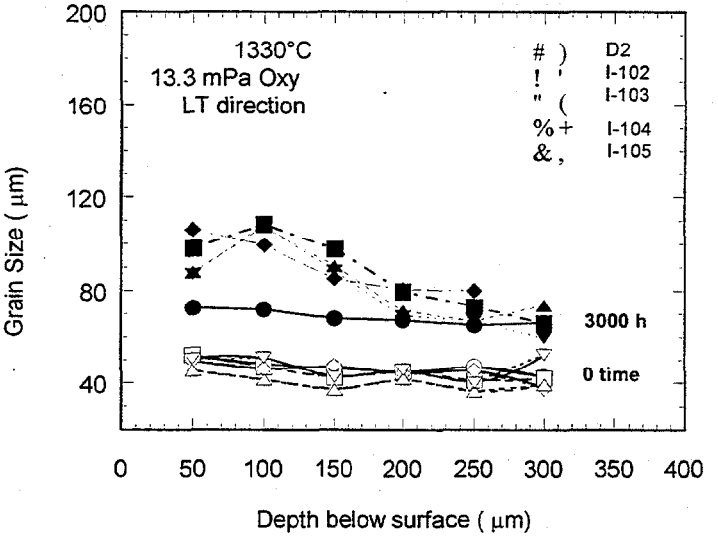

Fig. 3.10. Comparison of grain size as a function of depth below the surface of the sample for the Ce/Th-doped alloys and the new-process D2 DOP-26 alloy annealed at 1330°C in an oxygen partial pressure of 13.3 mPa.

3.2.2 References

1. E. P. George, p. 10 of "Quarterly Technical Progress Report of Radioisotope Thermoelectric Generator Materials Production and Technology Tasks for April through June 1995," ORNL/CF-95/66, Oak Ridge National Laboratory, Oak Ridge, TN, July 16, 1995.

2. J. W. Cohron and E. P. George, "Comparison of the Grain Growth Behavior of DOP-Ce and DOP-26 Iridium Alloys," attachment to letter from J. P. Moore to W. J. Barnett, Sept. 29, 1995.

3. A. N. Gubbi, E. P. George, E. K. Ohriner, and R. H. Zee, "Influence of Cerium Additions on High-Temperature-Impact Ductility and Fracture Behavior of Iridium Alloys," *Metall. Mater. Trans.* 28A, 2049-57 (1997).

4. C. G. McKamey, J. W. Cohron, and E. P. George, "Comparison of the Grain Growth Behavior of DOP-40 and DOP-26 Iridium Alloys," attachment to letter from J. P. Moore to W. J. Barnett, April 30, 1997.

5. E. P. George, E. K. Ohriner, and E. H. Lee, "Sensitivity of the High-Temperature Impact Ductility of DOP-40 Iridium to Small Changes in Ce and Th Concentration," attachment to letter from J. P. Moore to W. J. Barnett, Oct. 1998.

6. C. G. McKamey, E. H. Lee, E. P. George, and E. K. Ohriner, "Oxygen Compatibility of DOP-26 Iridium," attachment to letter from J. P. Moore to W. J. Barnett, April 24, 1992.

7. C. G. McKamey, A. N. Gubbi, E. H. Lee, E. P. George, and E. K. Ohriner, "Oxygen Compatibility of DOP-26, Ce-, Lu-, and Y-Doped Iridium Alloys at 1280°C and 1.3 mPa Oxygen Pressure," attachment to letter from J. P. Moore to W. J. Barnett, June 25, 1993.

8. C. G. McKamey, A. N. Gubbi, E. H. Lee, E. P. George, and E. K. Ohriner, "Compatibility of Old- and New-Process DOP-26 and Cerium-Doped Iridium Alloys at 1230°C and 1.3 mPa Oxygen Pressure," attachment to letter from J. P. Moore to W. J. Barnett, Aug. 29, 1994.

9. C. G. McKamey, J. W. Cohron, and E. P. George, "Oxygen Compatibility Studies of Old- and New-Process DOP-26 and Ce-Doped DOP-40 Iridium Materials at 1330°C and an Oxygen Partial Pressure of 13.3 mPa", attachment to letter from J. P. Moore to W. J. Barnett, Feb. 25, 1997.

10. C. G. McKamey and E. P. George, "Oxygen Compatibility of DOP-26 and DOP-40 Iridium Alloys at 1280°C and an Oxygen Partial Pressure of 13.3 mPa", attachment to letter from J. P. Moore to W. J. Barnett, March 27, 1998.

11. C. G. McKamey, E. H. Lee, J. W. Cohron, A. N. Gubbi, and E. P. George, "High-Temperature Low-Pressure Oxygen Compatibility of DOP-26 Iridium Alloys," attachment to letter from J. P. Moore to W. J. Barnett, Feb. 26, 1999.

12. C. G. McKamey, A. N. Gubbi, Y. Lin, J. W. Cohron, E. H. Lee, and E. P. George, *Grain Growth Behavior and High-Temperature High-Strain-Rate Tensile Ductility of Iridium Alloy DOP-26*, ORNL-6935, Oak Ridge National Laboratory, Oak Ridge, TN, April 1998.

13. J. J. Liao, Ph.D. Thesis, Auburn University, 1992.

14. J. W. Cohron, C. G. McKamey, and E. P. George, "Comparison of the Grain Growth Behavior of DOP-40 and DOP-26 Iridium Alloys," attachment to letter from J. P. Moore to W. J. Barnett, May 31, 1996.

15. C. L. White and C. T. Liu, *Acta Metall.* 29, 301 (1981).

16. C. G. McKamey, E. H. Lee, J. W. Cohron, and E. P. George, "The Effect of Low-Pressure Oxygen Exposure on the High-Temperature Tensile Impact Ductility of a Thorium-Doped Iridium Alloy," *Scripta Mater.* 35(2), 181-85 (1996).

17. C. G. McKamey, E. H. Lee, and E. P. George, "Oxygen Compatibility of Ce-doped Iridium Alloys at 1230°C and an Oxygen Partial Pressure of 13.3 mPa", attachment to letter from J. P. Moore to W. J. Barnett, Feb. 26, 1999.

18. C. G. McKamey, E. P. George, E. H. Lee, and E. K. Ohriner, "Effect of Grain Size on Impact Ductility in Ce+th-doped Dop-40 Iridium Alloys," attachment to letter from J. P. Moore to W. J. Barnett, January 31, 2000.

3.3 TECHNICAL SUPPORT FOR ADVANCED LONG TERM BATTERY

3.3.1 Background

The fuel in the Advanced Long Term Battery (ALTB) will be contained within nested capsules fabricated from Haynes 25. This material is a solid-solution cobalt-base alloy with excellent fabricability, corrosion resistance, and mechanical strength. Although the alloy was used several decades ago for fuel encapsulation, re-evaluation and qualification of a newly-produced heat was deemed an essential part of the safety test plan for the ALTB. Therefore a large heat of Haynes 25 was procured for testing and evaluation and to provide material for fuel encapsulation. ORNL was given the responsibility for measuring the mechanical properties needed for evaluating the lifetime of welded capsules under envisioned conditions of temperature, pressure and material aging. The test plan[1] called for uniaxially-stressed tensile, creep-rupture, and low-stress creep rate tests on base metal and weldments. As-received and aged materials were included in the test plan. In addition to the measurements on uniaxial specimens, the test plan included evaluation of aged and unaged capsules fabricated of Haynes 25 under various conditions of temperature and internal pressure. Data from this effort will also be compared to the historical data base and to previous models for the mechanical behaviour. More details of this effort and results on the tensile properties of unaged base metal were previously provided.[2]

3.3.2 Tensile Results

Base metal samples have been aged for 6000 h at a temperature of 675°C and another batch of tensile samples is being aged at 675°C for 12,000 h. Tensile measurements have been completed on the samples aged for 6000 h, and the results are given in Table 3.7. (These specimens are TT-BM-08 through TT-BM-14 in Table 2 of reference 1). Strength data are compared in Figure 3.11 to that from unaged base metal Haynes 25. As expected, aging increases both yield and ultimate strengths.

Table 3.7. Tensile properties of base metal Haynes 25 samples following aging for 6000 6 at 675°C

Test Temperature (°C)	Proportional limit (ksi)	Yield strength (ksi)	Ultimate strength (ksi)	Strain (%)		Reduction of area (%)
				Uniform	Elongation	
23	53	114.5	152.7	7.3	7.3	4.4
300	55	88.8	138.5	13.7	13.7	13.8
500	61	81.0	137.1	17.3	17.3	16.1
650	49	74.8	131.5	21.3	21.3	14.7
800	39	64.6	81.9	3.6	17.3	16.6
1000	-	25.8	25.9	-	45.2	39.0
1100	9	14.7	14.7	-	47.9	32.9

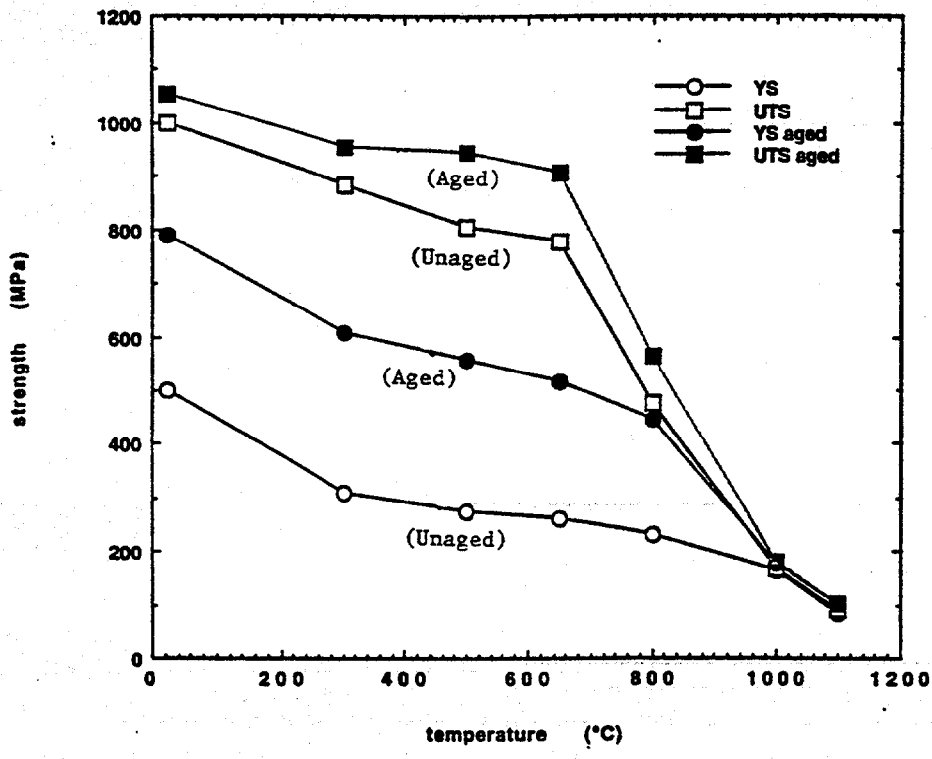

Fig. 3.11. Ultimate tensile strength (UTS) and yield strength (YS) of aged and unaged Haynes-25 as a function of temperature.

3.3.3 Creep-Rupture Testing

Four creep rupture specimens are currently under test as shown in Table 3.8. (The test numbers are from Table 3 in reference 1). As anticipated, none of these creep-rupture samples has failed yet.

Table 3.8. Uniaxial samples under creep rupture at the end of March 2000

Test no.	Temperature (°C)	Applied stress (psi)	Date started	Hours running	Failure hours
CR-BM-03	750	18,500	4/18/2000	~190	NA
CR-BM-04	800	14,400	3/23/2000	~190	NA
CR-BM-05	800	15,000	2/2/2000	~1400	NA
CR-BM-06	850	9,000	3/28/2000	~70	NA

3.3.4 References

1. M.F. McKittrick, Preliminary Safety Test Plan for the Advanced Long Term Battery (ALTB) Heat Source (HS), Teledyne Brown Engineering - Energy Systems, Hunt Valley, MD, April 30, 1999.

2. ORNL/CF-99/21, "Quarterly Technical Progress Report of Radioisotope Power System Materials Production and Technology Program Tasks for October 1998 Through March 1999" Edited by J.P.Moore.

3.4 B-SCAN AND ULTRASONICS

This effort has not yet been initiated.

4.0 PLUTONIUM PRODUCTION STUDIES

4.1 TARGET DEVELOPMENT

4.1.1 Dosimeter Targets

The objective of the dosimeter target irradiations is to characterize ^{238}Pu production, especially ^{236}Pu content, at various locations in each reactor. Dosimeter targets were designed, fabricated, and inserted into both the INEEL/ATR and the ORNL/HFIR. The resulting data will provide a firm basis for selection of appropriate ^{237}Np (n,2n) ^{236}Pu and ^{237}Np (γ, n) ^{236}Pu cross section data sets.

Six dosimeter capsules were irradiated and discharged from the ATR during this reporting period. Those capsules were shipped to ORNL late in March 2000 and will be subjected to isotopic analysis to determine ^{236}Pu content. Additional dosimeter targets will be discharged in March or April and shipped to ORNL in the fall of 2000.

Three dosimeter capsules were inserted into the HFIR and irradiated. Those capsules were cooled to allow activation products to decay and are currently undergoing chemical processing to recover the plutonium product.

4.1.2 Target Pellet Tests

A conceptual design for a test pellet was developed in conjunction with INEEL/ATR. ATR staff visited ORNL during January 2000 to assist in target design and provide input concerning relevant safety analyses. A conceptual design has also been developed for the ORNL/HFIR. The basic feature of the designs for target pellets is the use of an encapsulated mixture of Al and NpO_2 that has been compressed to ~80–90% of theoretical density in the form of a small pellet. Once several pellets have been fabricated, they can be inserted into a target capsule and irradiated.

As shown in Fig. 4.1, the pellet design uses a aluminum liner for the side walls of the cylinder and pressed aluminum caps for both ends. This encapsulation method was chosen in order to reduce contamination and potential pellet handling problems. (It should be noted that we anticipate future design of a prototype target without the aluminum liner in order to reduce waste aluminum.) The quantity of NpO_2 used in each pellet can be varied in order to provide data for various loadings of NpO_2. We anticipate this will allow determination of $^{236}Pu/^{238}Pu$ content over a spectrum of NpO_2 loadings.

The pressed pellets would then be inserted into an aluminum target. The target, depicted in Fig. 4.2 has been designed to accommodate multiple pellets so that multiple experiments can be accomplished in a single target. For these tests, we have chosen to insert eight pellets representing up to four different conditions (NpO_2 loadings) per target. The test uses four sets of two pellet pairs adjacent to each other as depicted in Fig. 4.3. The use of pellet pairs was chosen to allow greater quantities of 238Pu for analysis for a given NpO_2 loading and set of irradiation conditions. A dosimeter capsule is provided in the center of the target to allow characterization of the thermal and fast neutron fluxes.

A testing laboratory has been set up for development of NpO_2/Al pellets. For the early tests, a cerium oxide was selected as the cold surrogate for NpO_2. Initial pellet pressing was done with Al powder to determine the press pressure range needed to produce pellets to densities of 80% and 90%. Aluminum powders from three sources were acquired and evaluated. After initial scoping tests, Ce_2O_3 powder and the three samples of Al powder were mixed using a tumbler. In some cases, the powders did not mix well and the Ce_2O_3 powder appeared to segregate from the Al powder.

The Ce_2O_3 powder and Al powder were pressed to 80% and 90% density with a Ce_2O_3 loading of 80% by volume. The pellets were mounted in epoxy, cut open along the center line, and polished. In some cases, microscopic examination of the sectioned pellet revealed a poor Ce_2O_3-Al distribution. After examination of the pressed pellets, we modified our mixing techniques and selected the optimum Al powder. Several pellet tests performed using these modifications provided uniform distribution of cerium oxide in the pellets.

Three glove boxes were then prepared for hot pressing pellets with NpO_2. The glove boxes were decontaminated and equipped for the appropriate tasks. One glove box will be used to weigh and blend the powders. A new press is being fabricated to press 1/4-in. diam and 1/2-in.-diam pellets. A second glove box will be used to press and heat-treat the pellets. A vacuum oven is being fabricated to off gas the pellets and remove the stearic acid lubricant.

At the end of this reporting period, we are equipping an inert atmosphere glove box which will be used to perform closure welds of these targets. The use of He as an inert atmosphere was chosen to provide stronger QA support for the He leak tests for the final targets.

MCNP calculations for both reactors were initiated during this reporting period. The efforts on ATR have been focused on providing yield data to determine estimates of 238Pu content, fission product content, and heat generation rate for the NpO_2 loading conditions selected. The next step will be verification that thermal safety requirements for the ATR can be met and that shipping regulations can be met using the GE 100 cask. We anticipate two shipments between INEEL and ORNL and will need to verify that regulatory limits on dose rate and plutonium content will not be exceeded.

4.1.3 Waste Disposition

This effort begins with data from the FY1999 studies and looks at technologies for waste minimization proposed in the early study. Of particular interest, is the desire to segregate waste in order to minimize TRU waste and allow treatment of selected waste streams. The solid waste is further subdivided into porous and nonporous waste. These waste streams will require different approaches to waste pretreatment and minimizing action.

At this point, the molten salt oxidation (MSO) process has been identified as a potential baseline process for contaminated organic materials. Chemical and electrochemical decontamination has been identified for contaminated metal (nonporous) parts. We are currently investigating three methods of removing radioactive contamination from miscellaneous parts and equipment as a mechanism to eliminate a substantial portion of the non-porous radioactive waste. The three methods are (1) electrolytic decontamination, (2) chemical extraction with the TechXtract method, and (3) chemical oxidation with cerium (IV).

4.1.3.1 Electrolytic decontamination

Electrolytic decontamination is similar to electropolishing. The object being decontaminated is submersed in an electrolyte solution and becomes the positive electrode (i.e., cathode) for the process. Another metal object is also inserted into the electrolyte which serves as the negative electrode (i.e., anode). When a current is applied to the object, the surface layers of the object begin to dissolve. The removal of the surface layer also results in the removal of radioactive contamination.

A electrolytic cell has been setup to test the electrolytic decontamination method. The capability of the system will be assessed by beginning with noncontaminated items to determine the rate of surface removal, and then progress with increasingly contaminated items.

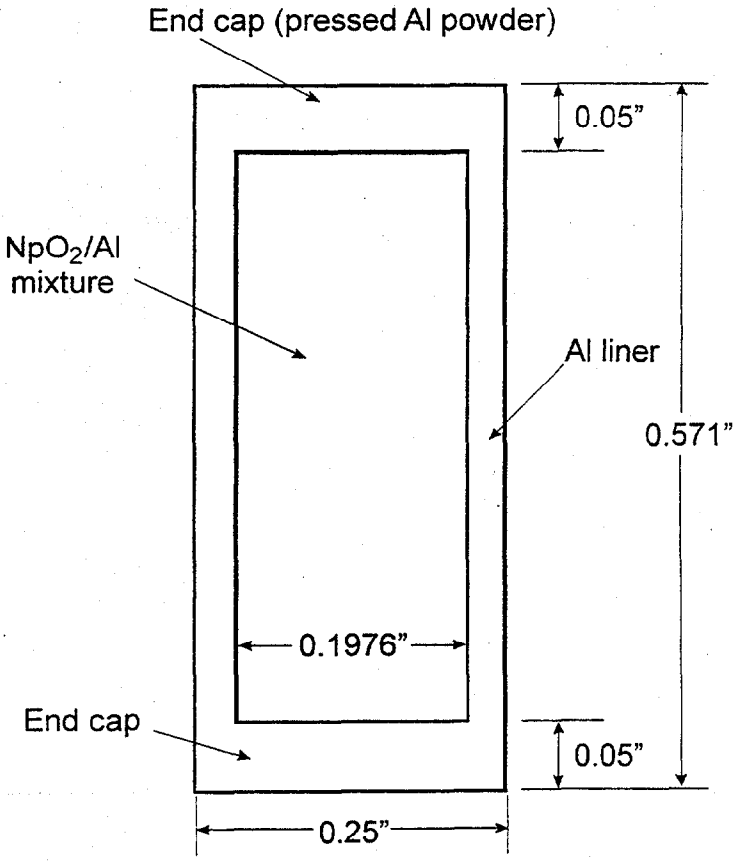

Fig. 4.1. Cylindrical pellet for actinide targets.

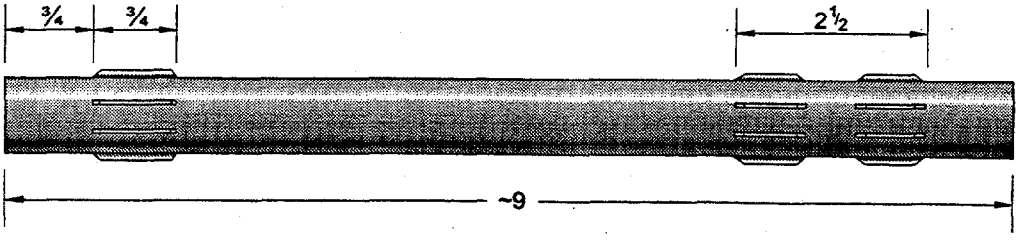

Fig. 4.2. Preconceptual ATR target design (dimensions are in inches).

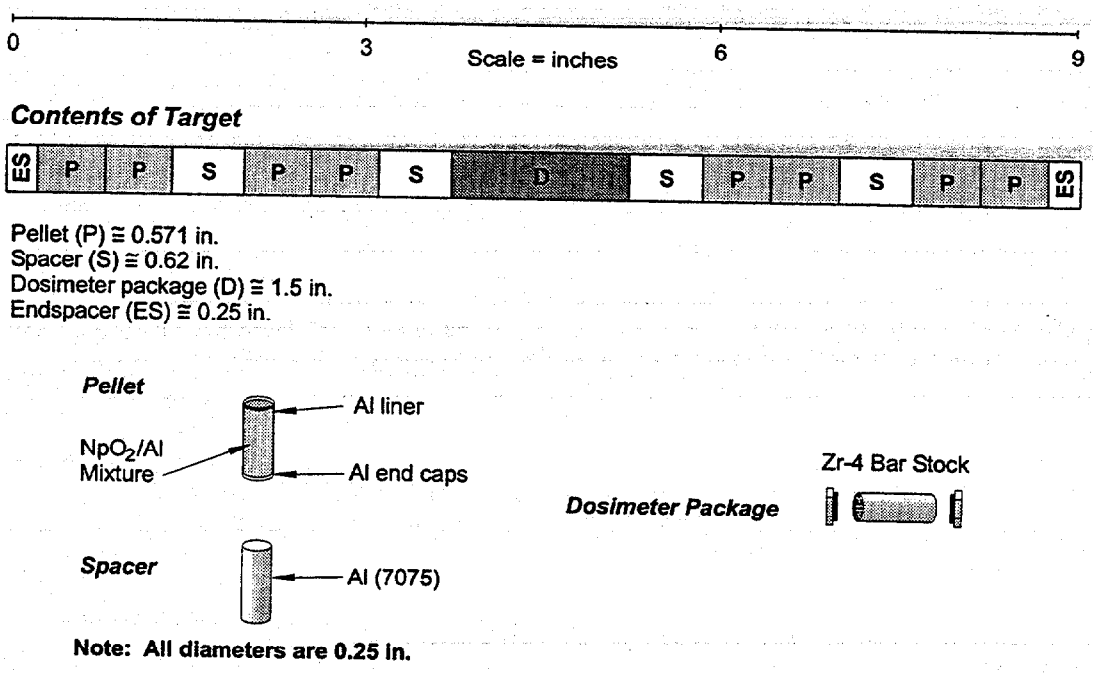

Fig. 4.3. Concepts for ATR pellet target.

4.1.3.2 Chemical extraction with the TechXtract method

The TechXtract process is a patented process for decontamination that is marketed by Active Environmental Technologies, Inc. Although the process was originally developed for removing polychlorinated biphenyls (PCBs) from materials, it has been shown to also be effective for removing radioactive contamination at other DOE sites. The process uses three chemical mixtures, which are marketed under the names TechXtract 0100, TechXtract 0200, and TechXtract 0300, and the exact composition of these mixtures is proprietary.

The TechXtract chemicals have been procured. The capability of the method will be determined by beginning with parts containing low levels of contamination and eventually progressing to higher levels.

4.1.3.3 Chemical oxidation with Cerium (IV)

The cerium (IV) oxidation decontamination process uses nitric acid solutions containing Ce^{4+} to oxidize and remove a few microns from the surface. This process releases and dissolves embedded radioactive contaminants from the surface.

Cerium (IV) oxide has been procured. Similarly to the other processes, the capability of this method will be assessed by beginning with materials that have low levels of contamination and eventually progressing to higher levels.

4.2 CONCEPTUAL PLANNING

4.2.1 Conceptual Design Studies

Most of the service lines in the proposed Plutonium Processing Facility (PPF) which run between in-cell and out-of-cell locations will be routed through unused viewing window cavities. Although there is probably sufficient space to route all such lines in this manner, some lines need to be routed through the existing 4" bent service tubes which originate on the Third Floor of Building 7930. This will be done in order to minimize congestion in the window areas, which will facilitate installation and subsequent replacement and repair of both in cell and out-of-cell lines, and also to take advantage of the convenient routing since some equipment will be located on the Third Floor of Building 7930. The concept is to route through the bent service tubes(1) most of the electrical and electronic instrumentation lines and (2) the pneumatic instrumentation lines which connect in cell tanks with out-of-cell transmitters.

Design concepts were developed to allow lines, electrical or tubing, to be routed through the 4-in. bent service tubes and then inside the hot call in a manner which allows them to be remotely replaced have been developed. These concepts should be utilized in the PPF because the large number of lines to be run precludes abandonment and rerouting through spare tubes. There is an additional cost associated, but this was estimated to be fairly small.

Recent design efforts focused on developing concepts for moving pellet targets out of the GE100 cask into the Building 7920 hot cells. An additional shielding plug will be needed for insertion into the GE100, which have an annular hole to allow removal of a basket containing the pellet targets. The shielding plug concept has been developed, and we are in the process of obtaining drawings of the GE100 to provide data for final design of the shielding plug.

Late in the reporting period, efforts on design studies were directed toward developing a design for interfaces to be used in an inert atmosphere glove box. The glove box will support milestones associated with pellet targets and has been discussed under item 4.1.2.

INTERNAL DISTRIBUTION

1. E. P. George
2. J. S. Ivey
3. J. F. King
4. C. G. McKamey
5-7. J. P. Moore
8. E. K. Ohriner
9. G. R. Romanoski
10. G. B. Ulrich
11. M. C. Vance
12. R. M. Wham
13. Laboratory Records
14-19. Laboratory Records, ORNL
20. ORNL Patent Office

EXTERNAL DISTRIBUTION

21-31. U. S. DEPARTMENT OF ENERGY, NE-50, Germantown Building, 11901 Germantown Road, Germantown, MD 20874-1290

W. J. Barnett
C. E. Brown
J. Dowicki
L. W. Edgerly
R. R. Furlong
L. C. Herrera
A. S. Mehner
W. D. Owings
R. C. Raczynski
L. L. Rutger
E. J. Wahlquist

32. DEPARTMENT OF ENERGY, Albuquerque Field Office, P.O. Box 5400, Albuquerque, NM 87115

R. L. Holton

33. DEPARTMENT OF ENERGY, Oak Ridge Operations Office, P.O. Box 2001, Oak Ridge, TN 37831

Assistant Manager, Laboratories

34-35. DEPARTMENT OF ENERGY, Oak Ridge Operations Office, Bldg. 4500N, Oak Ridge, TN 37831

L. W. Boyd, Mail Stop 6390
S. R. Martin, Jr., Mail Stop 6269

36. DEPARTMENT OF ENERGY, Los Alamos Area Office, 528 35th Street, Los Alamos, NM 87544

R. J. Valdez

37. DEPARTMENT OF ENERGY, Savannah River Operations Office, Bldg. 703F, P.O. Box A, Aiken, SC 29802

S. W. McAlhaney

38. DEPARTMENT OF ENERGY, Miamisburg Office, P.O. Box 66, Miamisburg, OH 45342

T. A. Frazier

39-40. BABCOCK AND WILCOX OF OHIO, INC., 1 Mound Road, Miamisburg, OH 45343-3000

D. M. Gabriel
J. R. McDougal

41-42. LOCKHEED MARTIN ASTRONAUTICS, P.O. Box 8555, Philadelphia, PA 19101

R. J. Hemler
R. M. Reinstrom

43. LOS ALAMOS NATIONAL LABORATORY, P.O. Box 1663, NMT-9, MS E502, Los Alamos, NM 87545

E. M. Foltyn

44. TETRA TECH NUS INC., 910 Clopper Road, Suite 400 Gaithersburg, MD 20878-1399

B. W. Bartram

44-45. ORBITAL SCIENCES CORPORATION, INC., 20301 Century Blvd., Germantown, MD 20874

R. T. Carpenter
E. A. Skrabek

46. PHILLIPS LABORATORY, Kirtland Air Force Base, AFRL/VSDV, 3550 Aberdeen Avenue SE, NM 87117

C. Mayberry

47. TELEDYNE BROWN ENGINEERING-ENERGY SYSTEMS, 10707 Gilroy Road, Hunt Valley, MD 21031

M. F. McKittrick

48. TEXAS A&M UNIVERSITY, Center for Space Power, Mail Stop 3118, College Station, TX 77843

M. J. Schuller

49. WESTINGHOUSE ADVANCED TECHNOLOGY BUSINESS AREA, P.O. Box 355, Pittsburgh, PA 15230-0355

M. O. Smith

50. WESTINGHOUSE SAVANNAH RIVER COMPANY, Savannah River Site, Aiken, SC 29808

R. W. Saylor